15. V. P. Glushko, L. V. Gurvich, et al., Thermodynamic Properties of Individual Substances [in Russian], Nauka, Moscow (1978).
16. I. G. Eremeitsev and N. N. Pilyugin, "Friction and heat exchange in laminar and turbulent boundary layers in nonequilibrium supersonic flow over axisymmetric bodies," Izv. Akad. Nauk SSSR, Mekh. Zhidk. Gaza, No. 2 (1984).

INTENSELY RADIATING, SUPERCRITICAL SHOCK WAVES

I. V. Nemchinov, I. A. Trubetskaya, and V. V. Shuvalov

UDC 533.6.011.72

The quasisteady structure of strong, intensely radiating shock waves propagating at a velocity D in a gas with a density ρ_0 and the laws of variation of their brightness temperatures T_ε with variation of D were investigated in [1, 2]. The role of emission is characterized by the parameter $\eta = q_b/q_h$, where q_b is the emission flux of a black body at the temperature T_s corresponding to the velocity D in accordance with the shock adiabat, q_h is the hydrodynamic flux of energy through the shock wave front, with $q_b = \sigma T_s{}^4$, while $q_h = (1/2)\cdot\rho_0 D u_s{}^2$ (σ is the Stefan–Boltzmann constant and u_s is the gas velocity behind the shock wave front). Subcritical (in the terminology of [1, 2]) shock waves, i.e., those for which $\eta < 1$, are usually used as emission sources [3].

Only the soft part of the radiation emitted by the gas behind the front travels to large distances from the front. The hard part of this radiation is absorbed immediately ahead of the front, forming a heated layer. In [1-3], the value I_1 of the first ionization potential of the working gas is taken as the arbitrary boundary ε_1 separating the spectrum into these parts. We note that, according to calculations [4, 5] and measurements [6, 7] of the total emission flux, ε_1 is 1-2 eV lower than I_1 owing to absorption in broadened lines in the heated layer. As the velocity D of the front and the parameter η increase, the maximum temperature T_- ahead of the wave front grows. Absorption also begins in the long-wavelength part of the spectrum. Only quanta emitted in the heated layer itself emerge. The brightness temperatures T_ε and the thermal-radiation fluxes q_r at first follow T_s and q_b and then, having reached maxima, decrease [1-7].

In subcritical shock waves the highest values of q_r and T_ε can be obtained by using helium and neon, which have the highest values of I_1, as the working gases. In neon, for example, according to calculations [4, 5] and measurements [6-8], they reach 9-10 eV and 200-400 MW/cm² at velocities of 50-70 km/sec. Higher temperatures T_s can be attained when heavier gases are used. The equation of state for xenon [9], for example, can be approximated by the power function

$$e = AT^{a}\delta^{-\alpha},\ \ \delta = \rho/\rho_L, \tag{1}$$

where e is the internal energy per unit mass, kJ/g; ρ and ρ_L are the density and standard density of xenon (5.89 mg/cm³); A = 4.0; a = 1.65; α = 0.14 in the temperature range T = 2-30 eV. Hence,

$$T_s = 0{,}35 u_s^{1{,}21}\delta_0^{0{,}085},\ \ \eta = 0{,}47\cdot 10^{-2} u_s^{1{,}81}\delta_0^{-0{,}66}. \tag{2}$$

Here u_s is in km/sec; T_s is in eV; $\delta_0 = \rho_0/\rho_L$. At a velocity u_s = 40 km/sec, according to (2), we obtain T_s = 30 eV for δ_0 = 1 and the back-body emission flux q_b is 88 GW/cm². In reality, however, shock waves are supercritical starting with u_s = 19 km/sec and T_s = 13 eV, while the maximum fluxes $q_r{}^m$ are already reached for subcritical waves and, according to [6, 7] comprise 15-20 MW/cm², corresponding to an effective temperature $T_e = (q_r{}^m/\sigma)^{1/4}$ = 3.0-3.5 eV. Thus, screening of the front prevents attaining high velocities and effective temperatures and obtaining large fluxes of radiation escaping from the front "to infinity."

Moscow. Translated from Zhurnal Prikladnoi Mekhaniki i Tekhnicheskoi Fiziki, No. 2, pp. 112-119, March-April, 1986. Original article submitted February 14, 1985.

0021-8944/86/2702-0260$12.50

The propagation of strong intensely radiating shock waves through a gas layer or cloud of limited size has been considered as one of the principles for weakening the screening effect [10-13]. After the front of the heated "tongue" arrives at the "boundary" between the cloud and the vacuum, radiation starts to escape almost freely. The flux density q_r of the emitted radiation proves to be of the order of magnitude of the hydrodynamic-flux density q_h, and hence $T_e \sim u_s^{3/4}\delta_0^{1/4}$. Thus, in principle, T_e and q_r as high as desired can be reached. For u_s = 40 km/sec, e.g., we obtain q_r = 19 GW/cm^2 and T_e = 21 eV. With a decrease in the density ρ_0 of the working gas it is easier to attain a given velocity D, but then the values of q_h and T_e decrease.

Let us estimate the characteristic thicknesses of the boundary layers. For supercritical shock waves, energy transfer in the heated layer has the character of radiative heat conduction [1, 2]. Neglecting effects of gas compression and motion in this layer, we write the energy balance for the quasisteady stage of the process of motion of the shock wave,

$$\rho_0 De(T_s, \rho_0) = -(16/3)\, l_R(T_s, \rho_0)\sigma T^3 \partial T/\partial x,$$

where ℓ_R is the Rosseland mean free path of the radiation. We approximate the dependence of ℓ_R on T and ρ by the power function

$$l_R = BT^b\delta^{-\beta}. \tag{3}$$

For xenon, b = 1, β = 1.7, and B = $1.8\cdot10^{-2}$ if ℓ_R is in cm while T is in eV. Using (1), we obtain the temperature distribution in the heated layer:

$$T/T_s = (1 - x/x_T)^{1/\omega}, \quad \omega = 4 - a + b.$$

Thus, a thermal wave develops ahead of a hydrodynamic shock [2]. The thickness x_T of the layer is determined through the expression

$$x_T = \frac{16}{3\omega}\frac{\sigma T_s^4}{q_h} l_R^s = \frac{16}{3\omega}\eta l_R^s, \; l_R^s = l_R(T_s, \rho_0).$$

Using Eq. (2), for xenon we have

$$x_T = 0.46\cdot10^{-4}u_s^{3.06}\delta_0^{-2.26}. \tag{4}$$

For u_s = 40 km/sec and δ_0 = 1, we find x_T = 3.6 cm. The value of x_T grows rapidly with an increase in u_s and a decrease in δ_0.

By using heavier gases than xenon, e.g., vapors of such metals as lead or bismuth, one can raise the temperature T_s and somewhat reduce the critical velocity u_s^* for which η = 1. Thus, for bismuth vapor at T = 2-30 eV, the constants in Eqs. (1) and (3) are A = 2.04, a = 1.82, α = 0.125, b = 1, β = 1.79, B = $0.83\cdot10^{-2}$, and ρ_L = 9.39 mg/cm^3. Accordingly, instead of (2) and (4) we obtain

$$T_s = 0{,}54u_s^{1{,}10}\delta_0^{0{,}069}, \; \eta = 1{,}87\cdot10^{-2}u_s^{1{,}40}\delta_0^{0{,}72},$$
$$x_T = 1{,}3\cdot10^{-4}u_s^{2{,}49}\delta_0^{-2{,}45}.$$

At low values of u_s (5-10 km/sec, let us say), T_s proves to be almost twice as high as for xenon. For δ_0 = 1, u_s^* = 17 km/sec, while T_s^* is the same as for xenon, 12 eV. At $u_s \approx$ 50 km/sec, the difference in T_s almost disappears, which is connected with the faster growth in the degree of ionization α_e, and hence in the quantity e, with temperature T.

At the same relative density δ_0, the switch to heavier elements having higher atomic weights and greater standard densities ρ_L leads to an increase in the absolute density ρ_0, and with it to a rise in q_h for a given velocity u_s. The fluxes q_r and effective temperatures T_e grow correspondingly for supercritical waves. Thus, for bismuth vapor at u_s = 40 km/sec and δ_0 = 1, q_h = 30 GW/cm^2 and T_e = 23 eV. Even so, in the regime of arrival of the radiating wave at the edge, T_e grows slower with an increase in D or u_s than does T_s, while q_r grows slower than q_b. This is connected with cooling of the gas behind the shock wave front when the radiation escapes freely. Temperatures close to T_s are maintained only in the region of optical depths of order $1/\eta$, and $T \to T_e$ far from the front. We shall show how to avoid such cooling.

Let us assume that two shock waves are propagating toward each other. After the boundaries of the heated layers are joined, a gradual rise in the temperature and radiation fluxes, up to values of the order of T_s and q_b, begins in the plane of symmetry.

Let the gas layer behind the shock wave fronts be optically thick, while the heated gas ahead of the shock wave fronts is almost transparent. It is obvious that most of the radiation emitted by one front falls again on the front of the opposite wave, and vice versa. Cooling is absent. Such a situation (opacity of the gas behind a front and transparency of that ahead of it) can be provided, in principle, since ℓ_R depends very strongly on ρ_0, while the compression behind the shock wave front is high (of the order of 10 in the absence of energy losses to emission and for an adiabatic index $\gamma = 1.2$). Accordingly, the mean free paths are far greater ahead of a front than behind it at the same temperature (about 50-fold). We note that if the thickness x_S of the layer between the shock wave fronts is small (less than the steady-state thickness x_T), then the wave structure differs from the quasi-steady-state structure. Under the condition that the gas is transparent or semitransparent, i.e., of the order of $\ell_R{}^S$ for x_S, the radiative transfer differs in its character from radiative heat conduction.

Shock waves with high velocities can be generated by the gas streams of explosive [14, 15] or magnetoplasma [16] compressors, as well as by foils accelerated to high velocities by laser beams [17, 18], by electron or ion accelerators [19], by electromagnetic implosion [20], or by other means [13, 21]. In the process of such acceleration, rigid foils are usually vaporized and gradually expand, their density decreasing in comparison with the density of the solid, while their thermal energy is far lower than their kinetic energy. We shall assume that the shock wave is generated by a cool gas layer, having a density ρ_1 higher than the density ρ_0 of the working gas in which it is decelerated, traveling at a high velocity. Heat fluxes from the hot plasma behind the shock wave front also heat the "foil" itself. The foil must have a relatively large mass so that the radiation cannot leak out through it. This is also required so that the velocity of the shock wave does not decrease too much from its initial velocity through deceleration in the working gas.

To allow for all these factors, we made direct calculations of the corresponding nonsteady radiative—gasdynamic problem. The calculation procedure is analogous to that used in [4, 5, 10-12]. It was assumed that at the initial time the shock waves were generated by the impact of two gas layers, of thickness $\Delta x = 0.5x_0$ and density $\rho_1 = 10\rho_0$, on the working gas of thickness $2x_0$ and density ρ_0. Thus, the mass $m_1 = \rho_1\Delta x$ of the "foil" is five times greater than the mass $m_0 = \rho_0 x_0$ of the gas decelerating its flight, and therefore the motion takes place without a significant loss of velocity. It was assumed that both the decelerating working gas and the "foil" gas consist of bismuth, and that they are cool at the initial time, i.e., their temperatures are far lower than T_S corresponding to the initial velocity u_0 of the foil. A shock wave with an initial velocity $D_0 = \frac{\gamma+1}{2}\frac{u_0}{1+\sqrt{\rho_0/\rho_1}}$, or with $D_0 = 0.84u_0$ and $u_S{}^0 = 0.76u_0$ for $\gamma = 1.2$ and $\rho_1/\rho_0 = 10$, propagates in the working gas as a result of the decay of the discontinuity.

Let us consider variants with relative densities $\delta_0 = 0.1$ and 1 for $u_0 = 50$ km/sec, in which case the mass m_1 of the foil is 6.6 and 66 mg/cm^2 while the initial kinetic energy is $E_0 = 8.2$ and 82 kJ/cm^2. The distributions of temperature T in the plasma at different times t are given in Fig. 1 (values of t in microseconds are indicated by the curves). For $\delta_0 = 0.1$ (Fig. 1a), the temperature proves to be equalized over the entire gas ahead of the front practically at once, and it rises gradually with time to the value $T_X = 34$ eV immediately before the reflection of the density jump. With an increase in δ_0 to 1 (Fig. 1b), the temperature rise at the center of symmetry occurs only after the arrival of the edge of the thermal wave, i.e., from the time t = 0.23 μsec.

In Fig. 2 we show the dependence on t of the unidirectional radiation flux densities $q_S{}^-$ and $q_S{}^+$ immediately ahead of the front in the heated layer, as well as the total flux density $q_S = q_S{}^- - q_S{}^+$ at the front and the unidirectional flux density q_r at the center of symmetry for $\delta_0 = 0.1$ (a) and $\delta_0 = 1$ (b). The highest unidirectional flux density q_X (by the time t_X of reflection) for $\delta_0 = 0.1$ is 13 GW/cm^2, which is about twice as high as q_h. For $\delta_0 = 1$, it grows to 220 GW/cm^2, which far exceeds both the hydrodynamic flux density q_h (four-fold) and the emission flux density q_b of a black body at $T_S{}^0 = 29$ eV (2.8-fold). We note that, just as for $\delta_0 = 0.1$, the value of q_X can be increased by increasing Δx and x_0 to values of the order of x_T.

If a small target is placed in the plane of symmetry, introducing a weak disturbance into the radiation field, the radiant flux incident on it will be close to q_r. The values

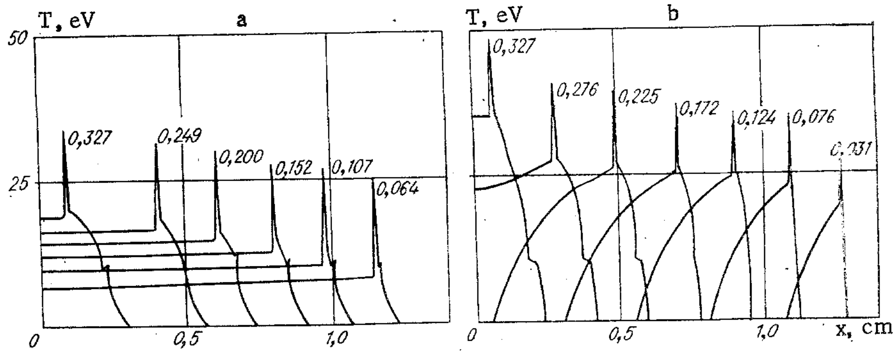

Fig. 1

of the energy $E_r = \int_0^{t_x} q_r dt$ are 2.5 and 6.0 kJ/cm² for δ_0 = 0.1 and 1. Thus, the conversion factors are $W = E_r/E_0$ = 30 and 7%. For δ_0 = 0.03 and 0.3, W = 2 and 25%, respectively.

If the reflection of a shock wave from an obstacle located in its path occurs rather than the collision of equal shock waves, then after the edge of the heated layer approaches the obstacle, the heating of its surface layer, vaporization, dispersion of the vapor, and its further heating by the incident radiation begin. As the temperature of the vapor increases, it radiates toward the shock wave, which decreases the cooling of the gas behind it. The expanding vapor generates a shock wave, moving opposite to the main one, in the working gas. The collision of such waves leads to an additional temperature rise and an increase in the radiation flux at the obstacle. The radiation temperatures and fluxes reached, however, are lower than in a symmetric collision. Thus, for u_0 = 50 km/sec and δ_0 = 0.1 we obtain q_x = 5 GW/cm² and T_x = 28 eV in the reflection. In this case, the characteristic pressure reached at the obstacle is already p_x = 0.9 GPa before the reflection of the wave.

If we analyze the radiative transfer in the one-group approximation and assume that the power-law approximations (1) and (3) are acceptable, then we can employ similarity considerations. Conserving geometrical similarity, i.e., the ratio $\Delta x/x_0$, as well as the ratio ρ_1/ρ_0 in the foil and in the decelerating gas, the degree of supercriticality of the shock wave at its initial velocity u_0 (i.e., the value of the parameter η_0) and the degree of transparency $x_0/\ell_R{}^0$ of the layer ahead of the wave, we can vary the density ρ_0, and with it the other parameters in accordance with the laws

$$\begin{gathered} u_0 \sim \rho_0^{0,517},\ x_0 \sim \rho_0^{-1,15},\ q_x \sim \rho_0^{2,55},\ E_0 \sim \rho_0^{0,88}, \\ m_1 \sim m_0 \sim \rho_0^{-0,15},\ t_x \sim \rho_0^{-1,67},\ T_s^0 \sim \rho_0^{0,64},\ p_x \sim \rho_0^{2,03} \end{gathered} \tag{5}$$

or

$$\begin{gathered} \rho_0 \sim u_0^{1,93},\ x_0 \sim u_0^{-2,22},\ q_x \sim u_0^{4,93},\ E_0 \sim u_0^{1,70}, \\ m_1 \sim m_0 \sim u_0^{-0,29},\ t_x \sim u_0^{-2,74},\ T_s^0 \sim u_0^{1,24},\ p_x \sim u_0^{3,93}. \end{gathered} \tag{6}$$

The ratio of the density ρ_{00} of the solid obstacle to the density ρ_0 of the gas could have figured as one more similarity criterion. In the heating and dispersion of vapor in a regime of developed screening, however, when the flux density is not too high, the initial density ρ_{00} of the material is not an important parameter, since the vapor density is far lower than ρ_{00}.

Now let us consider shock waves converging toward a target of radius r_0. Let the gas behind their fronts be optically thick. If the gas between the shock-wave front of radius r_s and the target is, on the contrary, transparent, while the target is small ($r_s \gg r_0$), then most of the radition emitted by the front arrives again at other sections of it, while a given section is heated by radiation emitted from all the other sections (a "light reactor"). The role of absorption of radiation by the target is small if $r_s{}^2 \gg r_0{}^2$. Inside the front, the radiation flux density q_r is close to $\sigma T_s{}^4$, and for supercritical shock waves it can be far higher than q_h. The condition of transparency of the gas ahead of the front is not obligatory in order for the flux incident on the target to be greater than q_h. It is important that radiative heat conduction be sufficiently strong.

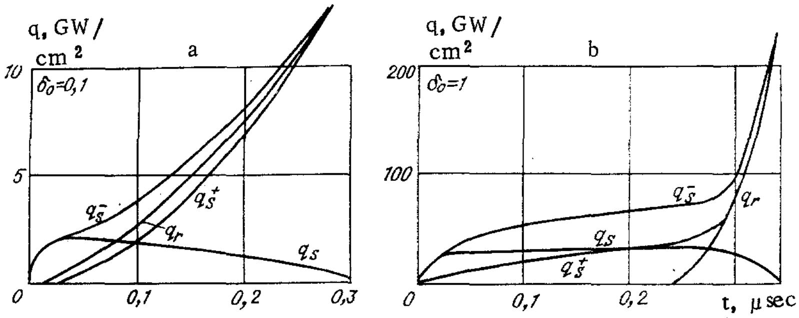

Fig. 2

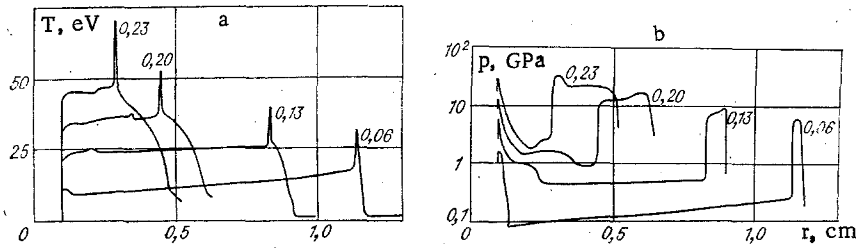

Fig. 3

The problem of the motion of a shell gathering toward the center and generating a converging shock wave, the gas ahead of which is transparent, has already been analyzed in [22] by estimates. A number of errors were committed in doing this. Thus, in determining the temperature of the gas in the region of its multiple ionization, expenditures on ionization were ignored and the adiabatic index γ was taken as 5/3. In determining the degree of "transmission" of radiation back through the shell, the density in it was taken as equal to the initial density, whereas in reality it falls greatly as the heated material expands. On the other hand, in determining the mean free paths of radiation, the plasma of heavy elements was taken as hydrogenlike, and absorption and emission in lines were ignored. Finally, it was assumed that the photon gas is compressed adiabatically as the radius of the transparent "cavity" decreases, leading to an increase in the radiation temperature. It is easy to show, however, that under the analyzed conditions ($\eta \leqq$ 10-100, $u_s \leqq$ 50-80 km/sec), the energy and pressure of the radiation are small compared with the thermal energy and pressure of the matter (they are less than 1-10%). Nevertheless, all this cannot discredit the very idea of using converging shock waves to increase the radiation fluxes at the target. Moreover, the idea of a light reactor can also be used under the conditions of partial transparency of the gas ahead of the front. It is also necessary to allow for effects of reradiation by target vapor and the motion of the secondary shock wave generated by the vapor.

In numerical calculations allowing for all these factors, we assumed that the shock wave is generated by a spherical gas shell having an initial density ρ_1 and velocity u_0, with an inner radius R_0 and an outer radius R_1. Inside the shell, down to the target of radius r_0, the stationary and cool gas has a constant density ρ_0. We assumed that the target, the shell, and the working gas are bismuth vapor. We used calculated data on their optical properties [9], obtained with allowance for bound–bound transitions, the actual (not hydrogenlike) structure of the atoms and ions, and the absorption cross sections, using functions determined by the Dirac–Fock–Slater method.

We give the results of calculations for u_0 = 50 km/sec with R_0 = 1.4 cm, $\Delta R = R_1 - R_0$ = 0.2 cm, and r_0 = 0.1 cm. These values are close to those adopted in [22], with the exception of ρ_0, which is lower in our calculations, since the time of arrival of the radiation at the obstacle will be too small otherwise. For $\rho_0 = 0.316 \cdot 10^{-2}$ g/cm^3 (or δ_0 = 0.3), the initial kinetic energy of the shell is E_k = 220 kJ and the mass of the shell is M = 0.17 g. In Fig. 3a, b we give the distributions over the radius r of the temperature T and pressure p, respectively, at different times t (the values of t in microseconds are given by the curves). The temperature ahead of the shock wave front gradually rises as it approaches the obstacle. The pressure at the vaporizing sphere, practically from the very start, proves to be close to the pressure at the front of the radiating shock wave and increases gradually with time. The

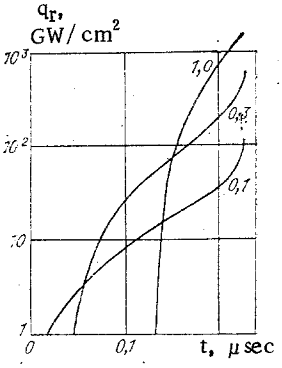

Fig. 4

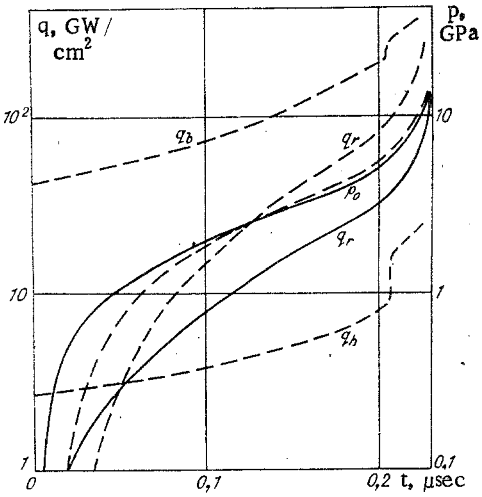

Fig. 5

radiation flux density q_x and the pressure p_x at the obstacle before the reflection of the shock wave are 210 GW/cm² and 14 GPa. For $\delta_0 = 1$ they already reach 1.2 TW/cm² and 52 GPa. Such values are far lower than those derived in [22], but still demonstrate the great possibilities of the method under consideration. For $\delta_0 = 0.1$, the values of q_x and p_x decrease to 35 GW/cm² and 6 GPa, which is noticeably higher than in the plane case, like the temperature T_x (40 eV instead of 34 eV). This is connected with weak effects of hydrodynamic cumulation.

The duration of the stage of high pressures and radiation flux densities shortens with an increase in δ_0. For $\delta_0 = 1$ it is only about 30 μsec (in Fig. 4 we show the time dependence of the flux to a sphere for different values of δ_0, indicated by the curves). This is connected with the fact that for high δ_0 the thermal wave moving ahead of the shock wave does not reach the target for a relatively long time. For the value $\delta_0 = 3$ adopted in [22], the corresponding time is shortened to about 2 nsec.

In Fig. 5 the solid lines are the results of a calculation of the variant with $\delta_0 = 0.1$, e.g., the values of the radiative flux density q_r incident on the target, the hydrodynamic energy-flux density q_h, the flux density q_b of the emission of a black body at the temperature T_s, and the pressure p_0 on the obstacle; the dashed lines are the results of a calculation for sizes R_0, R_1, and r_0 exceeding those indicated above by a factor of five (the time scale is altered accordingly). The character of the time variation of the pressure and its maximum value itself remain unchanged in the two cases, despite some variation in the maximum flux.

To scale these variants to other densities in the spherical case, one can use the same equations, (5) and (6), as in the plane case. In this case, the total energy $\mathscr{E}$ and the total mass M vary by the laws

$$\mathscr{E} \sim \rho_0^{-1,42} \sim u_0^{-2,74},\ M \sim \rho_0^{-2,45} \sim u_0^{-4,74}.$$

We note that the collision of the main shock wave with the secondary wave moving away from the target, leading to a spike of temperature and radiation flux, occurs at a rather large distance from the target (at a distance of the order of $2r_0$ under these conditions). Effects of hydrodynamic cumulation are weakly manifested by this time. The velocities of the wave and the shell vary insignificantly, so that effects of instability of the shock wave front and the ablation front propagating through the shell are hardly felt at all significantly.

The light-reactor effect should occur in the case of spherical or cylindrical symmetry of the converging waves, or for colliding plane waves, or when the surface geometry of the waves is more complicated. One of the advantages of using the method of deceleration, in the gas surrounding the target, of a shell accelerated to a high velocity, under conditions of strong radiative heat transfer to the target, is not only the possibility of attaining record temperatures and radiation fluxes, but also the possibility of using the effect of smoothing out and increasing the degree of symmetry of target irradiation in comparison with the degree of symmetry of the shell itself [23].

LITERATURE CITED

1. Ya. B. Zel'dovich and Yu. P. Raizer, "High-amplitude shock waves in gases," Usp. Fiz. Nauk, 63, No. 3 (1957).
2. Ya. B. Zel'dovich and Yu. P. Raizer, Physics of Shock Waves and High-Temperature Hydrodynamic Phenomena, Academic Press, New York (1967).
3. M. A. Tsikulin and E. G. Popov, Radiative Properties of Shock Waves in Gases [in Russian], Nauka, Moscow (1977).
4. E. G. Bogoyavlenskaya, I. V. Nemchinov, and V. V. Shuvalov, "Radiation of strong shock waves in helium at standard density," Zh. Prikl. Spektrosk., 34, No. 1 (1981).
5. E. G. Bogoyavlenskaya, I. V. Nemchinov, and V. V. Shuvalov, "Radiation of strong shock waves in neon at standard density," Zh. Prikl. Spektrosk., 36, No. 4 (1982).
6. Yu. N. Kiselev, "Total radiation yield from strong shock wave fronts in inert gases," in: Combustion and Explosion in Space and on Earth [in Russian], Izd. Vses. Astron.-Geod. Obshch., Moscow (1980).
7. Yu. N. Kiselev, "Emission of strong shock waves in inert gases in a wide spectral range," in: Proceedings of the Fourth All-Union Conference on Dynamics of a Radiating Gas [in Russian], Vol. 1, Mosk. Gos. Univ., Moscow (1981).
8. Yu. N. Kiselev, "Radiative properties of a strong shock wave in neon," Zh. Prikl. Mekh. Tekh. Fiz., No. 1 (1983).
9. M. A. El'yashevich, F. N. Borovik, S. I. Kas'kova, et al., "Thermodynamic functions and absorption coefficients of a bismuth–xenon plasma at temperatures of up to 30 eV," in: Proceedings of the Fourth All-Union Conference on Dynamics of a Radiating Gas [in Russian], Vol.1, Mosk. Gos. Univ., Moscow (1981).
10. V. I. Bergel'son and I. V. Nemchinov, "On the radiation generated by the impact of a gas layer against an obstacle at a very high velocity," Zh. Prikl. Mekh. Tekh. Fiz., No. 6 (1978).
11. I. V. Nemchinov and V. V. Shuvalov, "Emission of strong shock waves emerging at a boundary with a vacuum," Dokl. Akad. Nauk SSSR, 253, No. 4 (1980).
12. I. V. Nemchinov, I. A. Trubetskaya, and V. V. Shuvalov, "A spherical explosion with intense emission in a confined gas cloud," Dokl. Akad. Nauk SSSR, 276, No. 4 (1984).
13. T. Yabe and T. Mochizuki, "Impact radiative fusion concept," Jpn. J. Appl. Phys., 22, No. 4 (1983).
14. A. E. Voitenko, "Obtaining high-velocity gas jets," Dokl. Akad. Nauk SSSR, 158, No. 6 (1964).
15. Yu. N. Kiselev, K. L. Samonin, and B. D. Khristoforov, "Parameters of the jet of an explosive gas compressor," Zh. Prikl. Mekh. Tekh. Fiz., No. 3 (1981).
16. A. S. Kamrukov, N. P. Kozlov, and Yu. S. Protasov, "An investigation of processes of impact deceleration of hypersonic streams of dense plasma," Teplofiz. Vys. Temp., 16, No. 6 (1978).
17. Yu. V. Afanas'ev, N. G. Basov, O. N. Krokhin, et al., "Interaction of powerful laser radiation with a plasma," Itogi Nauki Tekh., 17 (1978).
18. S. P. Obenshain, R. R. Whitlock, E. M. McLean, et al., "Uniform ablative acceleration of targets by laser irradiation at 10^{14} W/cm^2," Phys. Rev. Lett., 50, No. 1 (1983).
19. M. B. Bavykin, "Electronic thermonuclear fusion," Itogi Nauki Tekh., Fiz. Plazmy, 2, Part 2 (1981).
20. Yu. D. Bakulin and L. V. Luchinskii, "Estimates of the possibility of obtaining high energy-flux densities in the electrical explosion of cylindrical shells," Zh. Prikl. Mekh. Tekh. Fiz., No. 1 (1980).
21. B. M. Manzon, "Acceleration of macroscopic particles for controlled thermonuclear fusion," Usp. Fiz. Nauk, 134, No. 4 (1981).
22. F. Winterberg, "Black-body radiation imploded inside a small cavity as an inertial confinement fusion driver," Z. Phys. A, Atoms Nuclei, 296, No. 1 (1980).
23. T. Mochizuki, S. Sakabe, and C. Yamanaka, "X-ray geometrical smoothing effect in indirect x-ray-drive implosion," Jpn. J. Appl. Phys., 22, No. 2 (1983).